A computer vision-based approach for respiration rate monitoring of group housed pigs

Meiqing Wang [a,b], Xue Li [a,c], Mona L.V. Larsen [a,d], Dong Liu [a], Jean-Loup Rault [e], Tomas Norton [a,*]

[a] Faculty of Bioscience Engineering, Katholieke Universiteit Leuven (KU LEUVEN), Kasteelpark Arenberg 30, 3001 Heverlee/Leuven, Belgium
[b] Animal Nutrition, Institute of Agricultural Sciences, ETH Zürich, Universit¨atstrasse 2, 8092 Zürich, Switzerland
[c] Institute of Agricultural Facilities and Equipment, Jiangsu Academy of Agricultural Sciences, Nanjing 210014, China
[d] Department of Animal Science, Aarhus University, Blichers Allé 20, DK-8830 Tjele, Denmark
[e] Institute of Animal Welfare Science (ITT), University of Veterinary Medicine (Vetmeduni) Vienna, A-1210 Vienna, Austria

ARTICLE INFO

Keywords:
Physiological monitoring
Oriented object detection
RGB video
Breathing
Animal welfare

ABSTRACT

In recent years, respiration rate (RR) monitoring using video data has been explored by researchers with relatively good success. However, the approaches used so far require the manual identification of the region of interest (ROI) in the image of the animal. When monitoring farm animals, typically housed in groups, such manual actions would entail an excessive time investment and increase the level of subjectivity in the application of the method. The aim of this study was to design a RR monitoring system targeted at group-housed animal applications. The developed system first selected video clips where pigs were in a resting status. Then an oriented object detector was used to detect each animal and select the ROI without manual intervention. Finally the RR is estimated by analyzing the time-varying features extracted from the ROI. Videos of group-housed pigs were collected to test the method, in which 5 pigs were included. Four pigs wore an ECG belt around the abdomen to collect the gold standard (GS) RR measures while a control pig did not wear a belt, with the GS for the control pig obtained through manually observation. The comparison between RR obtained by the computer vision (CV) method and the GS showed good agreement with a mean absolute error of 2.38 breath per minute (bpm) in the 4 pigs wearing belts and 1.72 bpm in the control pig, a root mean square error of 3.46 bpm in the 4 pigs wearing belts and 2.26 bpm in the control pig, and a correlation coefficient of 0.92 in the 4 pigs wearing belts and 0.95 in the control pig.

1. Introduction

Accurate measurement and monitoring of physiological parameters, such as body temperature, heart rate and respiration rate (RR), can have a wide range of applications when assessing animals' health and welfare (Sellier et al., 2014; von Borell et al., 2007). RR is of particular importance to identify early signs of heat stress and disease. For example, pleuropneumonia, a severe respiratory disease of pigs, can easily propagate across pigs causing weight loss and even death in affected pigs, impair pigs' health and increase the cost of production (Kerr et al., 2003). The main sub-clinical symptom of this disease is an increased RR (Opriessnig et al., 2011). Another example of RR in relation to welfare is heat stress. As pigs possess only limited sweat glands, they have limited thermoregulatory abilities and therefore are more sensitive to heat stress than other farm animals (Huynh, 2005). When the environmental temperature goes above the upper limit of their thermoneutral zone (around 17 – 21.5 ℃ for grower pigs at an age of 10–12 weeks), pigs dissipate heat by panting and their RR will increase immediately, followed by other undesirable effects, e.g., impaired immunity (Liu et al., 2021). Therefore, measuring and monitoring RR could potentially assist farmers in the detection of signs of infection or thermal discomfort at an early stage (Huynh, 2005; Jorquera-Chavez et al., 2021). As a result of having real-time measures of an animals' physiological state, farmers could take actions to safeguard the health or welfare problems of their animals with timely intervention or prevent the propagation of diseases.

Conventional techniques for monitoring RR for pigs usually require

* Corresponding author.
E-mail addresses: meiqing.wang@usys.ethz.ch (M. Wang), lixue@jaas.ac.cn (X. Li), monalilianvestbjerg.larsen@kuleuven.be, mona@anis.au.dk (M.L.V. Larsen), dong.liu@kuleuven.be (D. Liu), Jean-Loup.Rault@vetmeduni.ac.at (J.-L. Rault), tomas.norton@kuleuven.be (T. Norton).

human observation of flank movement (Brown-Brandl et al., 1998), which is a time consuming process and can be subject to inter- and intra-observer variability. Although sensors (such as respiratory belt transducers, electrocardiogram monitor, and photoplethysmography morphology) can replace human observation, these need to be in continuous contact with the skin of the animal (Eigenberg et al., 2002) and can cause undesirable skin irritation and discomfort for animals. In addition, contact sensors can be destroyed by penmates, due to their highly explorative nature of pigs. Novel contactless monitoring approaches are increasingly gaining attention as they can overcome these limitations. Moreover, recent advancements in camera and computer vision technologies have made it possible to monitor RR from videos (Massaroni et al., 2018a), while only a limited number of studies so far have attempted to measure and monitor RR in animals using videos (Barbosa Pereira et al., 2019; Jorquera-Chavez et al., 2021; Stewart et al., 2017). Three of these studies used infrared thermal (IRT) cameras to extract RR from images/videos (Barbosa Pereira et al., 2019; Jorquera-Chavez et al., 2021; Stewart et al., 2017). Even though using an IRT camera is effective in RR monitoring, this equipment is expensive and can suffer from a low signal-to-noise ratio depending on the environmental temperature. Compared to an IRT camera, RGB (Red Green Blue) cameras are more convenient as they are typically low-cost, easy to operate and have many other possible applications such as for analyzing animal behaviour (Chen et al., 2020; Liu et al., 2020), and heart rate monitoring (Wang et al., 2021).

Several methods have been adopted to extract the RR from videos, depending on the camera technology and region of interest (ROI). For methods using IRT videos, respiratory patterns can be extracted by capturing the temperature changes between the animal and its environment around the nostrils (Jorquera-Chavez et al., 2021; Stewart et al., 2017), and by analysing related pixel intensity changes around the chest based upon principle component analysis (PCA) (Barbosa Pereira et al., 2019). For methods using RGB videos, the extraction of RR is usually based on the imaging photoplethysmography (iPPG) principle, which assumes that changes in blood volume due to breath can cause different light absorptions on the skin surface, and the changes on the skin correspond to the changes in pixel intensity of the RGB channels (Sun & Thakor, 2015). Then, the respiratory patterns can be found by analysing the RGB signal from the ROI (Massaroni et al., 2018b; Nam et al., 2016). Even though RR has been successfully estimated by these methods, these studies all selected ROI manually, meaning that the monitoring system is not completely automatic. This cannot be conveniently applied to group-housed animals, as the ROI needs to be selected for each animal manually. This mainly results from the fact that the animal cannot be detected and localized accurately and automatically. To detect the animal in images of group-housed animals, recent studies have all used a rectangular frame-aligned bounding box to describe the location of the animal. Apart from the animal itself, this kind of bounding box contains a large amount of background pixels (mostly floor area), which are not useful to calculate to RR. Moreover, these studies only considered RR monitoring for a single pig instead of group-housed pigs, despite this being the most practically relevant housing environments for commercial pig production (Barbosa Pereira et al., 2019; Jorquera-Chavez et al., 2021; Stewart et al., 2017).

In this paper, we present an RGB video-based RR monitoring method for group housed pigs. The method used an oriented bounding box to localize the animal and capture the interface between the pig and the floor more accurately without including many irrelevant pixels. More specifically, the aim of this study was three-fold: (*i*) develop a measuring system capable of monitoring RR in real-time for group-housed pigs; (*ii*) integrate computer vision-based detection and signal analysis to extract RR with automated selection of ROI; (*iii*) explore the changes in automatically extracted RR for different individual pigs when the environmental temperature increases from 16 to 25 °C in 66–86 day-old pigs.

2. Materials and method

2.1. Animal experiment and data collection

The experiment was conducted in the animal experiment facilities (TRANSfarm) at KU Leuven during late February and early March of 2022. Five pigs (TN70 * PIC 408), at the age of 66 days, were included in the experiment. The pigs were group housed in one pen with a size of 2.90 m × 1.78 m (1.03 square meters per pig). A network camera (DH-SD1A203T-GN, Hangzhou, China) was located above the pen at the height of 2.5 m to capture the full pen area at a top-view angle (Fig. 1a). Video recordings of the animals were collected over day and night, with the infrared mode on during nighttime (from 1900 to 0800 h). The frame rate of the recordings was 25 fps. The only controlled factor in the experiment was temperature, which was simulated based on Belgium's daily summer temperature profile. The lowest temperature was set to 16 °C and the highest temperature was set to 25 °C. The temperature manipulation plan is illustrated in Fig. 1 (b). Humidity was not manipulated in the experiment, being in the range 45–60% during the experiments, which is suitable for growing pigs according to the Temperature and Humidity Index (THI) for growing pigs in the study of Lallo et al. (2018). A thermometer hygrometer was used to record the temperature and humidity during the experiment (Fig. 1a).

In order to collect the Gold Standard (GS) for RR, four wearable belts (Zephyr BioHarness 3, Annapolis, Maryland, USA) containing ECG devices were put around the pig abdomen 5 cm lower than the position of the heart. The belt measures RR based upon the principle of a strain gauge sensor embedded in the belt, which can capture the thoracic expansion and contraction causing size differentials that induce changes in capacitance because of resultant changes related to respiration (J.-H. Kim et al., 2013). The belt can record the RR of the animal every second with a range of 3 – 70 breaths per minute (bpm) and an accuracy of ± 1 bpm. One pig without a belt was kept as a control animal in order to rule out the effect of wearing the belt on calculating the RR through computer vision. In order to identify the animals, they were marked with numbers on the back using a livestock spray paint.

The experiment protocol did not require formal ethical approval when judged by the Ethical Committee for Animal Experiment, KU Leuven., while it was approved as an activity (No. M016/2021).

Forty video sequences (Mean duration ± Std: 2m24s ± 46 s) were selected from the video recordings, which included 4 cases: low temperature during day (LD), low temperature during night (LN), high temperature during day (HD) and high temperature during night (HN), with 10 video sequences for each case. The criteria of selecting the videos was based on all pigs in a status of resting. Fig. 2 illustrates 4 video frames representing each case. Note that each case was taken during a plateau of temperature.

2.2. Respiration rate extraction

To extract RR from the video automatically and exclude the effects from the belt, three steps were taken: (1) investigate the possibility of extracting RR from RGB video by manually selecting ROI, (2) extract RR in an automatic way by integrating a computer vision-based object detection method (Yi et al., 2021) with the RR extraction method in step 1, and (3) verify the automatic approach by ruling out the effects of the belt by comparing with data from the control pig not wearing a belt. The computation details in each step was illustrated in Fig. 3.

2.2.1. Step 1: Investigating the possibility of RR extraction from RGB video based on manually selected ROI

The extraction of RR in this study was based on capturing the periodic fluctuations around abdomen in continuous frames. Those fluctuations essentially are the intensity changes in the red (R), green (G) and blue (B) channels. Thus, the intensity changes over time at the edge of abdomen can be used to detect respiratory patterns. In order to

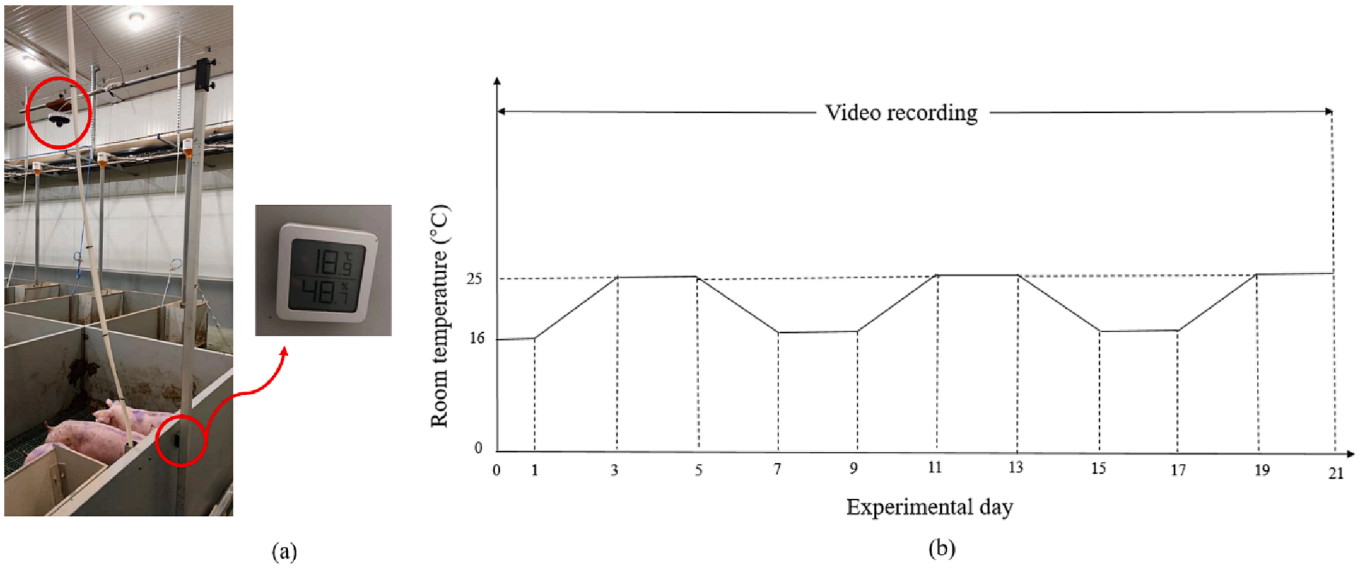

Fig. 1. (a) Illustration of the position of the camera (annotated by the top red circle) and the thermometer hygrometer (annotated by the bottom red circle); (b) plan of temperature schedule manipulation (in 21 days). (For interpretation of the references to colour in this figure legend, the reader is referred to the web version of this article.)

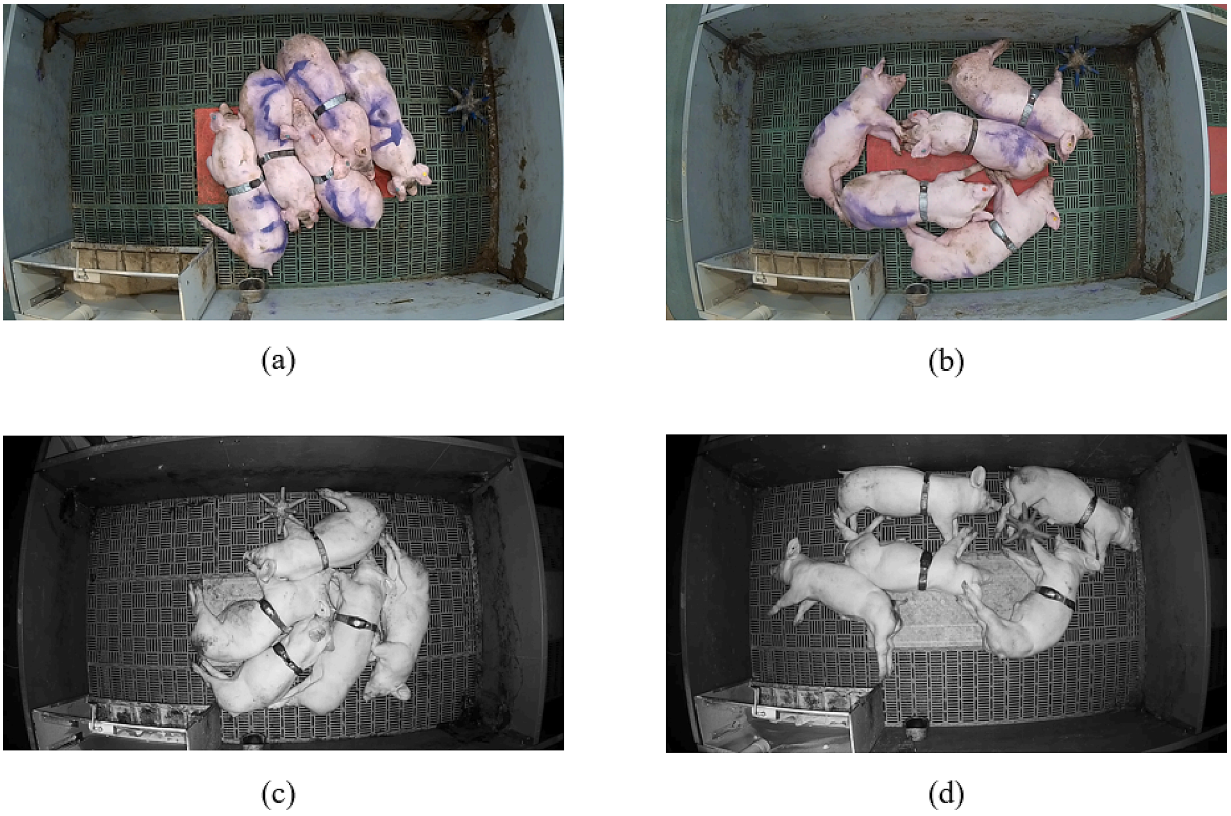

Fig. 2. Frame examples illustrating the four cases: (a) low temperature during day (LD); (b) high temperature during day (HD); (c) low temperature during night (LN); (d) high temperature during night (HN).

investigate the possibility of RR extraction from RGB video for pigs, we first manually selected regions around the abdomen with clearly visible periodic movements as ROI. Four video sequences were tested for manual ROI selection, one for each of the 4 cases: LD, HD, LN, HN. Fig. 4 illustrates the ROI selection in two frames for group-housed pigs.

The pseudo-code of RR extraction is given in Algorithm 1. In the selected ROI, the R, G and B intensity of each pixel $I(x, y, c, t)$ were first summed up in each frame, represented by $s_{pixel}(x,y,t)$. Because each pixel in the ROI is a function of t, the extracted intensity of the pixel is a time series of values over a certain video segment. Then each $s_{pixel}(x, y)$ was detrended by Z-score normalization (normalizing every value in a time series such that the mean of all of the values is 0 and the standard deviation is 1). After that, the standard deviation (std) of each $s_{pixel}(x, y)$ was computed, and the top 5% of pixel intensities with the highest std

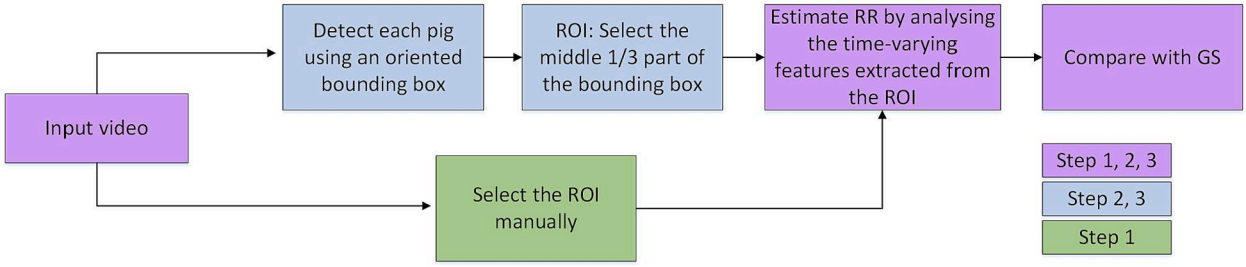

Fig. 3. Flowchart illustrating the computation details in the 3 steps.

Fig. 4. Frame examples illustrating manual ROI selection in the case of LD and HN.

were selected as candidates (defined as ROI in Algorithm 1) for analyzing RR given that the intensity variation is caused by respiration. The mean value of the selected candidates was then computed (defined as MROI in Algorithm 1). To remove the noise, a ten-point moving average filter and bandpass filter with frequency range 0.25–2 Hz were applied (defined as $ROI_{filtered}$). The frequency range was determined by the normal RR (25 to 40 bpm) of weaned pigs (Pereira et al., 2019). In order to compute the RR, the first derivative of the filtered signal was calculated ($definedas ROI_{der}$), then all zero-crossing points in the first derivative signal were found out (defined as ROI_{zero}). The time between every two odd zero-crossing points was considered as the time for one inhale-exhale respiration cycle. The extracted RR was compared with GS by performing Pearson correlation and regression analysis. Considering the length of videos and the computation of RR timely, a sliding window (60 s) with a moving step (5 s) was adopted in the comparison, meaning that both the RR extracted from the video and the RR obtained from the belt were averaged over the time window.

Algorithm 1: Computation details of RR extraction

Assume: the intensity of the pixel at the position (x, y) in frame t is $I(x,y,c,t)(c = R,G,B)$, the summed intensity of pixel (x, y) in frame t is $s_{pixel}(x,y,t)$, the time series of pixel (x, y) in the video is $s_{pixel}(x,y)$, the normalized time series of pixel (x, y) in the video is N $s_{pixel}(x,y)$, the selected pixel time series is ROI, the mean of selected pixel time series is MROI, the filtered MROI is $ROI_{filtered}$, the first derivative of $ROI_{filtered}$ is ROI_{der}, the detected zero-crossing points in ROI_{der} is ROI_{zero}, the respiration rate at detected zero-crossing points is RR.

Input: Video v

for t in v:
  for pixel (x, y) in fame t:
    $s_{pixel}(x,y,t) = \sum_{c=R,G,B} I(x,y,c,t)$
  $s_{pixel}(x,y) = \text{append}(s_{pixel}(x,y,t))$
for time series of pixel $s_{pixel}(x,y)$ in v:
  N $s_{pixel}(x,y) = \text{zscore}(s_{pixel}(x,y))$
ROI $= sort_{top5\%}(std(Ns_{pixel}))$
MROI = mean(ROI)
$ROI_{filtered}$ = filter (MROI)
$ROI_{der} = ROI'_{filtered}$
$ROI_{zero} = detect(ROI_{der})$
for i in ROI_{zero}:

(*continued on next column*)

(*continued*)

RR(i) $= 60/(ROI_{zero}(i+3) - ROI_{zero}(i+1))$

Output: Respiration rate RR.

Note that append(·) represents appending the value to the series, and filter(·) includes moving average and bandpass filter.

2.2.2. Step 2: Towards an automatic computer vision approach

With the aim of automatically measuring RR over RGB videos in the second step, an object detection algorithm (Yi et al., 2021) and the RR calculation method in Step 1 were integrated. The object detection algorithm was pre-trained to detect objects using an oriented bounding box for 40 epochs on the DOTA dataset (Xia et al., 2018) and 100 epochs on the HRSC2016 dataset (Liu et al., 2017). This pre-trained model was fine-tuned in this study using 123 frames from 40 video recordings, wherein every pig was labelled by an oriented bounding box via the labelImg labelling tool (https://github.com/chinakook/labelImg2). The training took about 30 min with 50 epochs and batch size of 4. The inference speed was 11.62 fps on frames with a size of 1920 * 1080 pixels. The speed was measured on a single NVIDIA GeForce RTX 3090 GPU. In addition, the computation speed to extract the RR in Step 1 using manually selection of ROI was 283.88 fps. Following the common practice of object detection, the training accuracy was evaluated by mean Average Precision (mAP), which was defined based on the Intersection over Union (IoU) method. Ten IoU thresholds (0.5: 0.05: 0.95) were used to evaluate the model and the model achieved 0.99 in mAP@0.5 and 0.87 in mAP @[0.5:0.95]. The details of accuracy in different thresholds can be found in Table 1. The fine-tuned model was then adopted to infer the location of pigs over the video recording. Fig. 5 (a) shows a frame example illustrating the detection of individual pigs. To exclude large motion artefacts that usually appear around the head and tail, the middle third of the bounding box was further selected as ROI. Fig. 5 (b) illustrates the automatic selection of ROI. After that, the computation of RR was the same as described in Step 1. Finally, the results were compared with the GS by performing Pearson correlation and Bland Altman analysis. Forty video sequences were included in the test of the computer vision-based RR monitoring.

Table 1
Accuracies of detection in different thresholds.

Threshold	0.50	0.55	0.60	0.65	0.70	0.75	0.80	0.85	0.90	0.95
Accuracy	0.99	0.99	0.99	0.99	0.99	0.99	0.99	0.95	0.71	0.12

Fig. 5. Frame examples of: (a) detection result represented by the green bounding boxes; (b) automatically ROI selection represented by the red bounding boxes. (For interpretation of the references to colour in this figure legend, the reader is referred to the web version of this article.)

2.2.3. Step 3: Verification on the control pig without a belt

It was found that the time series of intensity values for the selected pixels were mostly around two regions: the interface between the abdomen and floor, and the edge of the belt. Fig. 6 shows the selected pixels with higher std for RR extraction. As introducing the belt was intended to collect the GS, it cannot be avoided that the movements related to RR were more clear around the belt due to the contrast difference between belt and skin. Therefore, to exclude the effect of the belt, a control pig without a belt was used to verify the extraction method. That also means that the GS could not be obtained from the belt for this individual. Nevertheless, as mentioned before, the respiration of pigs is visible around the abdomen. The RR was collected by observing the video and counting the fluctuations around the abdomen, a method already verified by Jorquera-Chavez et al. (2021). Thus, the GS for the pig without a belt was obtained by observing the video. A total of 40 video sequences were tested in the verification. Note that the window size and moving step adopted in the observation were the same as the computation in the video.

Table 2 shows the summary of video sequences that were used in each step.

2.3. Comparison of individual RR changes at different room temperatures

It is known that pigs behave differently during day and night, e.g., pigs are more active during day and increase lying time during night (Ekkel et al., 2003). In addition, pigs tend to have a higher RR in active

Table 2
Summary of the videos sequences used in each step.

Step	Number of videos	Number of pigs	Mean duration	Std duration
1	4	16 (4 × 4)	2m09s	24 s
2	40	160 (4 × 40)	2m24s	46 s
3	40	40 (1 × 40)	2m24s	46 s

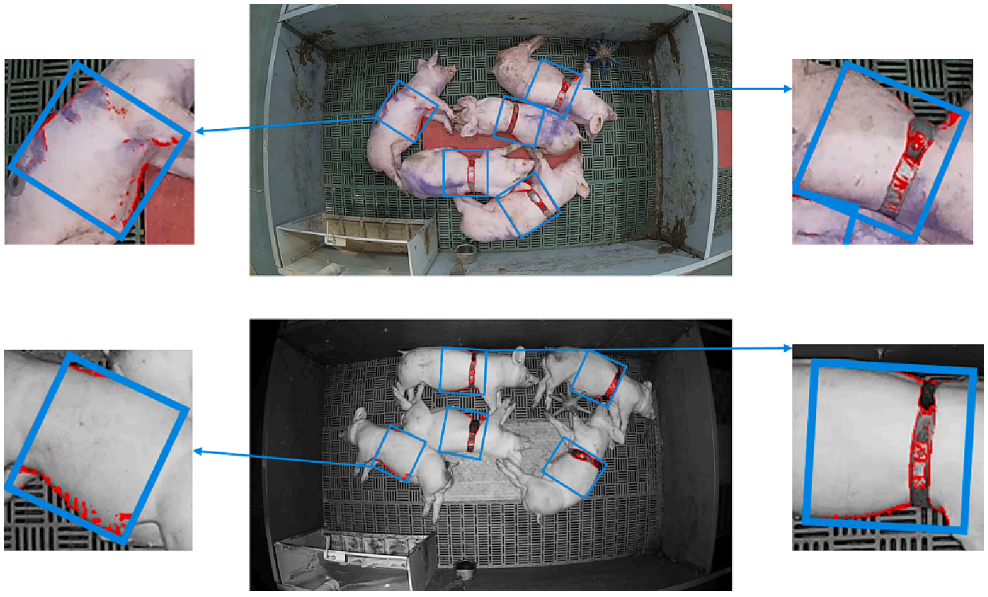

Fig. 6. Frame examples illustrating the selected pixels for RR extraction. The selected pixels for RR extraction were marked in red, and the ROI was marked using a blue bounding box. (For interpretation of the references to colour in this figure legend, the reader is referred to the web version of this article.)

than in resting status (Costa et al., 2013). Thus the RR is likely to be different during the day and night as well. Given that the ambient room temperature was the only manipulated factor in this study and pigs usually show increase in RR as temperature increases, we hypothesized that there would be some interaction between time (day/night) and room temperature on the RR of the pigs. To verify this, a statistical analysis based on a linear mixed model (Bates, 2005) was conducted with pig identity as random effect in the model. The statistical model included time (day/night), temperature (16/25 °C) and their interaction as fixed effects. Note that the analysis was based on the RR extracted by CV averaged per video (n = 40). The statistical analysis was conducted in the R software (R Core Team, 2022) using the packages '*lme4*' (Bates et al., 2015) for model estimation and '*emmeans*' (Lenth et al., 2022) for post hoc analysis.

3. Results and discussion

In the following text, the abbreviations CV_m and CV_a are used to denote the results obtained by manually and automatically selecting ROI, respectively. GS_m and GS_a indicate that the GS was obtained by manually observation and the belt respectively.

3.1. Results for manual ROI selection

The mean (MROI) and filtered ($ROI_{filtered}$) signal of all selected pixels in ROI for the case of HD are shown in Fig. 7(a)(b) respectively. The respiratory patterns can already be seen in the MROI signal. We can see from Fig. 7(b) that the respiratory patterns are clearer in the filtered signal $ROI_{filtered}$. Fig. 7(c) shows the first derivative of $ROI_{filtered}$, where we can see an even clearer respiratory pattern. The comparison of the extracted RR and the GS can be found in Table 3. It shows a strong correlation between the GS and CV-obtained RR (r = 0.93). The low mean absolute error (MAE) and root mean square error (RMSE) also show the effectiveness of the extraction method, which proves that it is possible to extract RR from RGB videos for pigs.

3.2. Results for automatic ROI selection

Table 4 shows the comparison between RR extracted by CV versus GS. The value of MAE and RMSE show low estimating error, even better than when the ROI was selected manually. The correlation coefficient in Table 4 and regression result in Fig. 8(a) show a strong correlation with the GS. Besides, the Bland Altman plot (Fig. 8(b)) illustrates a good agreement between RR obtained from the CV and GS methods. For Fig. 8 (a) and (b), although there are some RR extractions outside the 95% confidence interval, the results still show very strong positive correlation and agreement between the GS and CV-based methods, which means the automatic ROI selection method can extract RR from RGB video reliably.

Table 3
Comparison of respiration rate extracted by computer vision (CV) with the gold standard (GS) for which the ROI is selected manually (step 1).

Method	Range (bpm[1])	Mean	MAE (bpm[1])	RMSE (bpm[1])	Correlation Coefficient (r)
CV_m	(18.41, 53.66)	31.64	2.50	3.90	0.93***
GS_a	(17.70, 57.15)	32.69			

*** ($p < 0.001$).
[1] bpm: breaths per minute.

Table 4
Comparison of respiration rate extracted by computer vision (CV) versus the gold standard (GS) when the ROI is selected automatically (step 2).

Method	Range (bpm[1])	Mean	MAE (bpm[1])	RMSE (bpm[1])	Correlation Coefficient (r)
CV_a	(16.14, 65.60)	31.27	2.38	3.46	0.92***
GS_a	(13.60, 65.68)	31.38			

*** ($p < 0.001$).
[1] bpm: breaths per minute.

3.3. Results from the control pig

The automatic RR extraction method developed in Step 2 was further tested on the control pig to rule out the effect of wearing the belt on the measurement. The comparison of the GS and the CV-extracted RR are shown in Table 5, Fig. 9, where it can be seen that the automatic extraction also worked for the control pig, not depending on the belt.

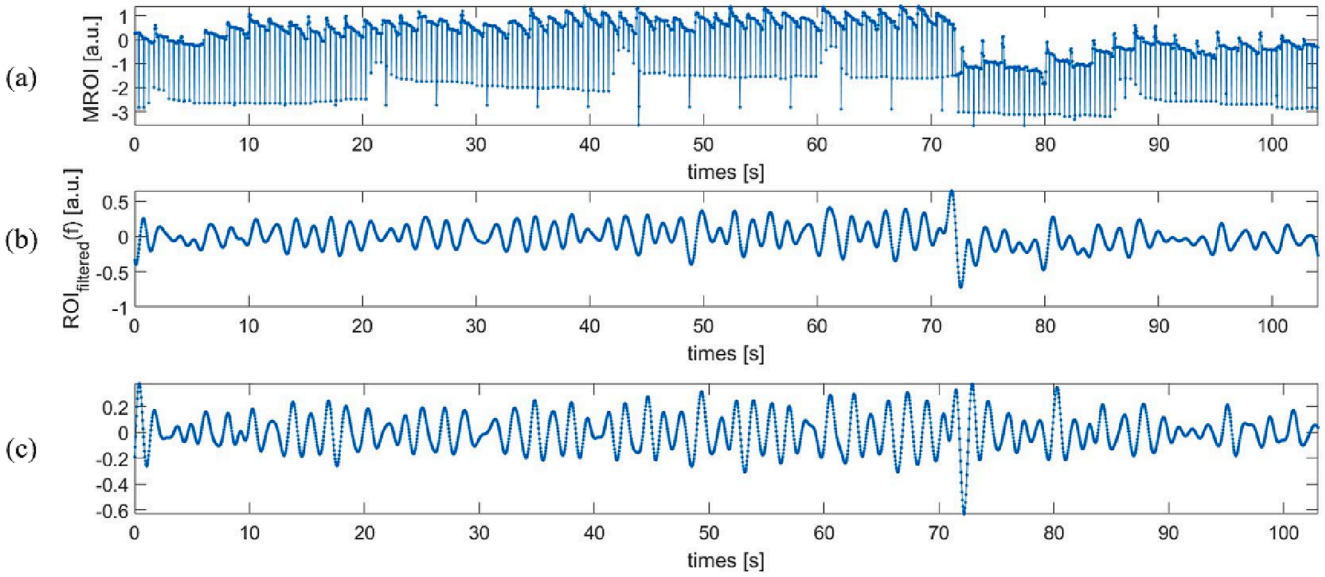

Fig. 7. Case HD: (a) the mean signal of all selected pixels in manually selected ROI, (b) the filtered signal of all selected pixels in manually selected ROI, (c) the first derivative of $s_{filtered}(f)$.

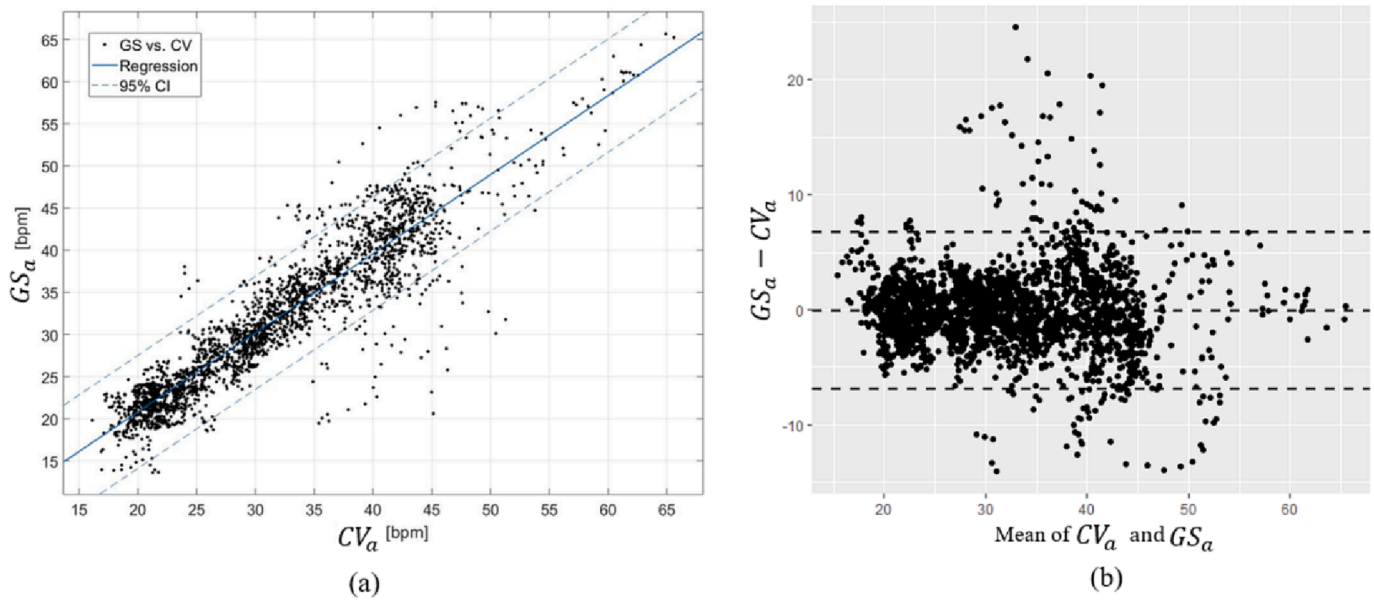

Fig. 8. Four pigs with belts (Step2): (a) regression analysis of the relationship between respiration rate (RR) obtained from gold-standard (GS_a) and computer vision (CV_a)-based methods (95% CI: 95% confidence interval; bpm: breaths per minute); (b) Bland Altman plot showing the difference between respiration rate (RR) obtained from gold standard GS_a and computer vision (CV_a)-based methods. The three dash lines represent the 95% confidence intervals and the mean of the difference between GS_a and CV_a.

Table 5
Comparison of respiration rate (RR) extracted by computer vision (CV) with the gold standard (GS) for the control pig (without the belt) when ROI was selected automatically (step 3).

Method	Range (bpm[1])	Mean	MAE (bpm[1])	RMSE (bpm[1])	Correlation Coefficient (r)
CV_a	(16.38, 44.61)	31.27	1.72	2.26	0.95**
GS_m	(13.87, 45.83)	26.86			

** ($p < 0.001$).
[1] bmp: breaths per minute.

Note that the difference between Fig. 9 and Fig. 8 is the number of data points: this figure shows the results obtained from the control pig, while Fig. 8 shows the results of the 4 pigs wearing the belt, which has 4 times of data points compared to this figure.

Similar to the present study, Jorquera-Chavez et al. (2021) investigated the use of a CV method to extract RR in pigs, where IR images were recorded to identify the temperature changes around the nose and human observation was used as GS. Nevertheless, the reported agreement between the GS and the CV-based extraction was not as good as in the present study (r = 0.61–0.66). Also similar to the study of Jorquera-Chavez et al. (2021), Pereira et al. (2019) also used IRT imagery to measure RR for anesthetised piglets, where the GS was obtained by an anesthesia machine and capnography. That study reported very good agreement (MAE averaged = 0.27 ± 0.48 bpm) between the GS and their IRT-based method. However, the animals in that study were anesthetized, meaning that the recordings did not involve large motion artefacts and the methodology proposed did not consider variable conditions present in typical living environment. Stewart et al. (2017) used IRT images to extract the RR in cattle, and reported very good agreement between the GS and CV-based methods. However, the method for assessing RR was based on the observation of the recordings and manual counting of air movement from the nostrils, which cannot be considered automatic monitoring.

3.4. Changes in individual RR with ambient room temperature

A significant interaction was found between time (day/night) and temperature (16/25 °C) ($P < 0.05$; Fig. 10 (a)). It can be seen that the RR was numerically higher at 25°than that at 16°, which was in line with the findings from previous studies (Huynh et al., 2005; Kim et al., 2009). However, this difference was only significant during the night. Although the difference in low and high temperature during day and night has not been explored yet, it has been reported that pigs follow a circadian rhythm generally, including both physiology and behaviour changing periodically during 24 h (Ingram & Dauncey, 1985). Given that pigs are more active in the day than in the night (Ingram & Dauncey, 1984), it is counter-expected that the RR is higher at the high temperature during the night. A further analysis on individual level showing the RR difference for each pig between low and high temperature during night was conducted and the results can be seen in Fig. 10 (b). For pig 1, the estimated RR was 28.41 bpm higher in high than in low temperature during the night, implying that this pig was more affected by the heat during the night, which indicates that different pigs have different physiological responses to heat exposure.

It is expected that animals have individual differences in behavioural and physiological responses towards environmental changes. For instance, the formation of social hierarchy in piglets was determined by individual differences in sibling competition (D'Eath, 2005), and cows have individual differences in heat tolerance (Bun et al., 2017). In the light of the development in Precision Livestock Farming, focus on animals' health and welfare have been increasingly moved to individual instead of group level and the current results elucidate the importance of this move. Considering the observed differences in RR towards heat exposure for different pigs, the method in this study has great potential to identify pigs with high heat tolerance to cope with global climate change.

3.5. Limitations and future working points

The limitations of this study arise mainly from motion artefacts, which can corrupt the signal such that the time-varying features related to respiratory patterns is unrecoverable. The video where pigs were in

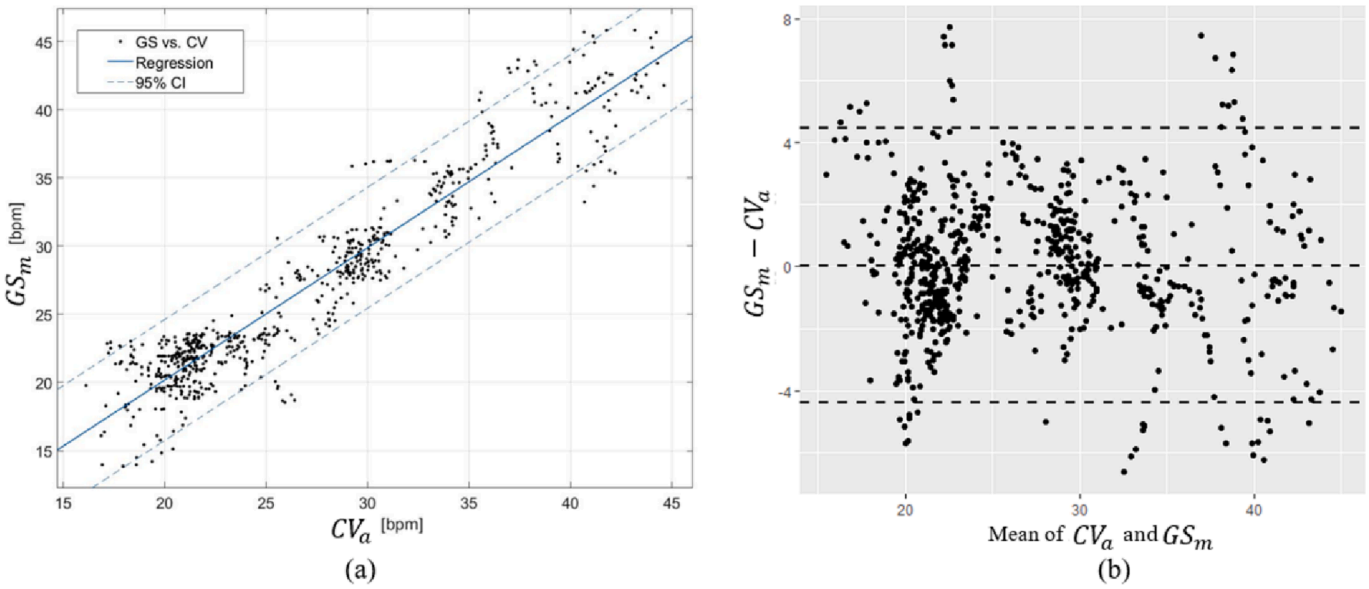

Fig. 9. The control pig not wearing the RR monitoring belt (Step3): (a) regression analysis of the relationship between respiration rate (RR) obtained from manual observation as gold standard (GS_m) and computer vision (CV_a)-based methods for the control pig (95% CI: 95% confidence interval; bpm: breaths per minute); (b) Bland Altman plot showing the difference between respiration rate (RR) obtained from gold standard (GS_m) and computer vision (CV_a)-based methods. The three dash lines represent the 95% confidence intervals and the mean of the difference between GS_a and CV_a.

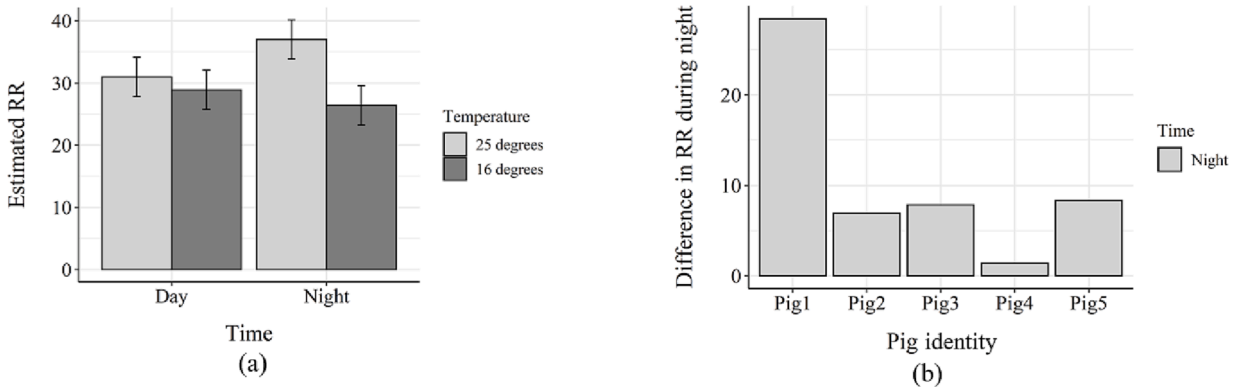

Fig. 10. (a) Model estimated respiration rate (RR) at different temperatures during day and night; (b) Averaged RR difference for each pig between low and high temperature during night (Pig 5 is the control pig not wearing the belt).

resting status and did not move were selected to extract RR, thus the method in this study is not applicable to cases where pigs move. Therefore, monitoring the RR for non-resting pigs could be an important working point in future. However, this could be very challenging considering the difficulties in finding out the respiratory patterns from motion artefacts. In addition, only the case where all the 5 pigs did not move were included in this study. Nevertheless, in most farm applications some pigs may be resting while others are moving. Therefore, future research could also focus on detecting which pigs are resting and then utilizing the developed method to monitor the RR.

4. Conclusion

A computer vision-based method was developed that allows automatic measurements of respiration rate for group-housed pigs. The method consisted of an oriented object detector to automatically select the region of interest, followed by analysis of the time-varying features to extract respiration rate from this region. The comparison between respiration rate obtained by computer vision and the gold standard method showed strong agreement: MAE, RMSE and correlation coefficient values of 2.38, 3.46 and 0.92, respectively, from four pigs wearing belts, and values of 1.72, 2.26 and 0.95, respectively from a control pig not wearing a belt, but in which the respiration rate was measured from manual observations. Besides, the statistical analysis for respiration rate revealed differences between high and low ambient room temperatures, and between day and night time, showing that pigs react differently to heat exposure. Based on the encouraging results from this study, future work can move forward to apply the automated respiration rate monitoring approach in applied settings to investigate the relation between respiration rate and animals' health and welfare on an individual level in group-housed animals.

CRediT authorship contribution statement

Meiqing Wang: Conceptualization, Methodology, Validation, Formal analysis, Investigation, Data curation, Writing – original draft, Writing – review & editing, Visualization, Project administration. **Xue Li:** Investigation, Writing – review & editing. **Mona L.V. Larsen:** Conceptualization, Formal analysis, Writing – review & editing, Supervision. **Dong Liu:** Methodology, Formal analysis, Writing – review & editing. **Jean-Loup Rault:** Writing – review & editing, Supervision. **Tomas Norton:** Conceptualization, Project administration, Supervision,

Resources, Funding acquisition, Methodology, Writing – review & editing.

Declaration of Competing Interest

The authors declare that they have no known competing financial interests or personal relationships that could have appeared to influence the work reported in this paper.

Data availability

Data will be made available on request.

Appendix A. Supplementary data

Supplementary data to this article can be found online at https://doi.org/10.1016/j.compag.2023.107899.

References

Barbosa Pereira, C., Dohmeier, H., Kunczik, J., Hochhausen, N., Tolba, R., Czaplik, M., Gao, C.-Q., 2019. Contactless monitoring of heart and respiratory rate in anesthetized pigs using infrared thermography. PLoS One 14 (11), e0224747.

Bates, D., 2005. Fitting linear mixed models in R. R News 5 (1), 27–30.

Bates, D., Mächler, M., Bolker, B., Walker, S., 2015. Fitting linear mixed-effects models using lme4. ArXiv Preprint ArXiv:1406.5823.

Brown-Brandl, T.M., Nienaber, J.A., Turner, L.W., 1998. Acute heat stress effects on heat production and respiration rate in swine. Trans. ASAE 41 (3), 789.

Bun, C., Watanabe, Y., Uenoyama, Y., Inoue, N., Ieda, N., Matsuda, F., Tsukamura, H., Kuwahara, M., Maeda, K., Ohkura, S., 2017. Evaluation of heat stress response in crossbred dairy cows under tropical climate by analysis of heart rate variability. J. Vet. Med. Sci. 17–368.

Chen, C., Zhu, W., Steibel, J., Siegford, J., Han, J., Norton, T., 2020. Recognition of feeding behaviour of pigs and determination of feeding time of each pig by a video-based deep learning method. Comput. Electron. Agric. 176, 105642.

Costa, A., Ismayilova, G., Borgonovo, F., Viazzi, S., Berckmans, D., Guarino, M., 2013. Image-processing technique to measure pig activity in response to climatic variation in a pig barn. Anim. Prod. Sci. 54 (8), 1075–1083.

D'Eath, R.B., 2005. Socialising piglets before weaning improves social hierarchy formation when pigs are mixed post-weaning. Appl. Anim. Behav. Sci. 93 (3–4), 199–211.

Eigenberg, R.A., Brown-Brandl, T., Nienaber, J.A., 2002. Development of a respiration rate monitor for swine. Trans. ASAE 45 (5), 1599.

Ekkel, E.D., Spoolder, H.A.M., Hulsegge, I., Hopster, H., 2003. Lying characteristics as determinants for space requirements in pigs. Appl. Anim. Behav. Sci. 80 (1), 19–30.

Huynh, T.T.T, 2005. Heat stress in growing pigs. Wageningen University and Research.

Huynh, T.T.T., Aarnink, A.J.A., Verstegen, M.W.A., Gerrits, W.J.J., Heetkamp, M.J.W., Kemp, B., Canh, T.T., 2005. Effects of increasing temperatures on physiological changes in pigs at different relative humidities. J. Anim. Sci. 83 (6), 1385–1396.

Ingram, D.L., Dauncey, M.J., 1984. Carbohydrate-induced thermogenesis and its modification by the beta-blocker propranolol. Comp. Biochem. Physiol., C: Comp. Pharmacol. Toxicol. 77 (1), 23–27.

Ingram, D.L., Dauncey, M.J., 1985. Circadian rhythms in the pig. Comp. Biochem. Physiol. A Physiol. 82 (1), 1–5.

Jorquera-Chavez, M., Fuentes, S., Dunshea, F.R., Warner, R.D., Poblete, T., Unnithan, R. R., Morrison, R.S., Jongman, E.C., 2021. Using imagery and computer vision as remote monitoring methods for early detection of respiratory disease in pigs. Comput. Electron. Agric. 187, 106283.

Kerr, C.A., Eamens, G.J., Briegel, J., Sheehy, P.A., Giles, L.R., Jones, M.R., 2003. Effects of combined Actinobacillus pleuropneumoniae challenge and change in environmental temperature on production, plasma insulin-like growth factor I (IGF-I), and cortisol parameters in growing pigs. Aust. J. Agr. Res. 54 (10), 1057–1064.

Kim, B.G., Lindemann, M.D., Cromwell, G.L., 2009. The effects of dietary chromium (III) picolinate on growth performance, blood measurements, and respiratory rate in pigs kept in high and low ambient temperature. J. Anim. Sci. 87 (5), 1695–1704.

Kim, J.-H., Roberge, R., Powell, J.B., Shafer, A.B., Williams, W.J., 2013. Measurement accuracy of heart rate and respiratory rate during graded exercise and sustained exercise in the heat using the Zephyr BioHarnessTM. Int. J. Sports Med. 34 (06), 497–501.

Lallo, C.H.O., Cohen, J., Rankine, D., Taylor, M., Cambell, J., Stephenson, T., 2018. Characterizing heat stress on livestock using the temperature humidity index (THI)—prospects for a warmer Caribbean. Reg. Environ. Chang. 18 (8), 2329–2340.

Lenth, R., Singmann, H., Love, J., Buerkner, P., Herve, M., 2022. Estimated marginal means, aka least-squares means. R package version 1.7.4-1. J. Stat. Softw. 69, 1.

Liu, F., Zhao, W., Le, H. H., Cottrell, J. J., Green, M. P., Leury, B. J., Dunshea, F. R., Bell, A. W., 2021. What have we learned about the effects of heat stress on the pig industry? Animal, 100349.

Liu, D., Oczak, M., Maschat, K., Baumgartner, J., Pletzer, B., He, D., Norton, T., 2020. A computer vision-based method for spatial-temporal action recognition of tail-biting behaviour in group-housed pigs. Biosyst. Eng. 195, 27–41.

Liu, Z., Yuan, L., Weng, L., Yang, Y., 2017. A high resolution optical satellite image dataset for ship recognition and some new baselines. Int. Conf. Pattern Recognit. Appl. Methods 2, 324–331.

Massaroni, C., Lopes, D.S., Lo Presti, D., Schena, E., Silvestri, S., 2018b. Contactless monitoring of breathing patterns and respiratory rate at the pit of the neck: a single camera approach. J. Sens. 2018, 1–13.

Massaroni, C., Schena, E., Silvestri, S., Taffoni, F., Merone, M., 2018a. Measurement system based on RBG camera signal for contactless breathing pattern and respiratory rate monitoring. IEEE Int. Sympos. n Med. Measur. Appl. (MeMeA) 2018, 1–6.

Nam, Y., Kong, Y., Reyes, B., Reljin, N., Chon, K.H., Yang, Y., 2016. Monitoring of heart and breathing rates using dual cameras on a smartphone. PLoS One 11 (3), e0151013.

Opriessnig, T., Giménez-Lirola, L.G., Halbur, P.G., 2011. Polymicrobial respiratory disease in pigs. Anim. Health Res. Rev. 12 (2), 133–148.

Pereira, C.B., Dohmeier, H., Kunczik, J., Hochhausen, N., Tolba, R., Czaplik, M., 2019. Contactless monitoring of heart and respiratory rate in anesthetized pigs using infrared thermography. PLoS One 14 (11).

R Core Team, 2022. R: A language and environment for statistical computing. R Foundation for Statistical Computing, Vienna, Austria. Http://Www. R-Project. Org/.

Sellier, N., Guettier, E., Staub, C., 2014. A review of methods to measure animal body temperature in precision farming. Am. J. Agric. Sci. Technol. 2 (2), 74–99.

Stewart, M., Wilson, M.T., Schaefer, A.L., Huddart, F., Sutherland, M.A., 2017. The use of infrared thermography and accelerometers for remote monitoring of dairy cow health and welfare. J. Dairy Sci. 100 (5), 3893–3901.

Sun, Y., Thakor, N., 2015. Photoplethysmography revisited: from contact to noncontact, from point to imaging. IEEE Trans. Biomed. Eng. 63 (3), 463–477.

von Borell, E., Langbein, J., Després, G., Hansen, S., Leterrier, C., Marchant-Forde, J., Marchant-Forde, R., Minero, M., Mohr, E., Prunier, A., Valance, D., Veissier, I., 2007. Heart rate variability as a measure of autonomic regulation of cardiac activity for assessing stress and welfare in farm animals – a review. Physiol. Behav. 92 (3), 293–316. https://doi.org/10.1016/j.physbeh.2007.01.007.

Wang, M., Youssef, A., Larsen, M., Rault, J.-L., Berckmans, D., Marchant-Forde, J.N., Hartung, J., Bleich, A., Lu, M., Norton, T., 2021. Contactless video-based heart rate monitoring of a resting and an anesthetized Pig. Animals 11 (2), 442.

Xia, G.-S., Bai, X., Ding, J., Zhu, Z., Belongie, S., Luo, J., Datcu, M., Pelillo, M., Zhang, L., 2018. DOTA: A large-scale dataset for object detection in aerial images. In: Proceedings of the IEEE Conference on Computer Vision and Pattern Recognition, 3974–3983.

Yi, J., Wu, P., Liu, B., Huang, Q., Qu, H., Metaxas, D., 2021. Oriented object detection in aerial images with box boundary-aware vectors. In: Proceedings of the IEEE/CVF Winter Conference on Applications of Computer Vision, 2150–2159.